Holographic Dendrogramic Theory: predictability of relational dynamics of the event universe and the emergence of time arrow

Oded Shor [2,3], Felix Benninger [1,2,3], and Andrei Khrennikov [4,*]

[1] Department of Neurology, Rabin Medical Center, Petach Tikva, Israel

[2] Felsenstein Medical Research Center, Beilinson Hospital, Petach Tikva, Israel

[3] Sackler Faculty of Medicine, Tel Aviv University, Tel Aviv, Israel

[4] Faculty of Technology, Department of Mathematics Linnaeus University, Växjö, Sweden

Abstract. Recently we started the development of *Holographic Dendrogramic Theory* (DH-theory). It is based on the novel mathematical representation of the relational event universe (in the spirit of (Smolin, Barbour, Rovelli). Elementary events are represented by branches of dendrograms, finite trees, which are generated from data with clustering algorithms. In this note we study the dynamics of the event-universe generated by the appearance of a new event. Generally, each new event can generate the complete reconstruction of the whole dendrogramic universe. However, we found (via numerical simulation) unexpected stability of this universe. Its events are coupled via the hierarchic relational structure which is relatively stable with respect even random generation of new events. We also observe the regularity patterns in location of new events on dendrograms. In the curse of evolution, the dendrogram's complexity increases and determine the arrow of time the event universe. We use the complexity measure from particle shape dynamics which was shown to be increase in both direction away from a Janus point and thus determine the arrow of time in symmetrical manner away from a Janus point. The particle shape dynamics theory is a relational theory with close ideological resemblance to DH-theory as both relays on Mach's principle and Leibniz's relationalism and his principles. By using the complexity measure on dendrograms and its p-adic string representation, we demonstrate the emergence of time arrow from the p-adic zero-dimensional field, where space and time are absent.

Keywords: event-universe, dendrograms, hierarchic relational representation, dendrogramic dynamics, shape dynamics, stability of event-universe, arrow of time

1.Introduction

In the series of papers [1-3], we developed basics of *Holographic Dendrogramic Theory* (DH-theory).This theory grew up from information physics (starting with Wheeler's "it from bit" [4]) and relational event representation of the universe(Smolin, Barbour, Rovelli [5-13]). The latter approach was combined with methods of p-adic theoretical physics in which physical structures are represented by p-adic numbers.[1] In contrast to the main stream, we explore not the number theoretical methods, but the

[1] See [16-29] for applications to strings and quantum theory; see [30-32] for applications to disordered systems (spin glasses).

 doi:10.20944/preprints202204.0193.v1

treelike geometry in that p-adic numbers (see Appendix A) are visualized as the branches of the p-adic tree (the homogeneous tree with p>1 edges leaving each vertex).[2]

In DH-theory, the elementary events such as outcomes of measurements are represented by the branches of a finite tree, so-called *dendrogram*.[3] The latter by itself represents a complex event combined of elementary events. A dendrogram can be generated from experimental data with the aid of a hierarchic *clustering algorithm*.[4] One of the aims of development of DH-theory is to merge classical and quantum descriptions; the same dendrogramic description of events is used in both cases. The degree of classicality and quantumness of events is characterized by dendrogram's size, increasing of size is treated as increasing of classicality (see, e.g., [2] for application to the violation of CHSH inequality). The merging of the classical and quantum descriptions might lead to the resolution of the problem of creation of quantum gravity.

In complete accordance with *ontic-epistemic approach* to science [42-47], DH-theory has two counterparts. The epistemic one is devoted to special (hierarchically relational) structuring of knowledge obtained by an observer from experiments. The ontic one gives the mathematical model of "the universe as it is". In our theory the epistemic and ontic descriptions are naturally coupled: they are based on finite and infinite trees, respectively. This paper is based on the results of numerical simulation, and we would not concern the ontic model (cf. [1-3]). The epistemic counterpart of DH-theory is briefly presented in section 2, a few words about its ontic counterpart are said in section 3.

In this note we study the dynamics of the event-universe generated by the appearance of a new event. Generally, each new event can generate the complete reconstruction of the whole dendrogramic universe. The elementary events created up to the moment t=k are hierarchically ordered via the dendrogram's structure. And the appearance of a new event at t=k+1 can, in principle, destroy the previous hierarchic structure. The dynamics which is local in the physical space becomes nonlocal in dendrogram-space. Thus, all events are permanently in dynamical motion; an event which had happened a milliard years ago is not frozen at same point of the dendrogram-space, contemporary events disturb it and vice versa: the position of newly generated event in the dendrogram-space is determined by all previously occurred events. The dendrogram-universe is in the permanent motion and recombination.

Nevertheless, this event-motion has some degree of regularity and stability. The appearance of a new event does not generate a totally random redistribution of events. Only very special dendrogramic configurations can be created with high probability. The presence of the hierarchic relational structure in the event-universe

Total recombination of the events and the change of the structure of the event-universe also can happen, but with relatively small probability (a kind of catastrophic perturbation of the otherwise stable hierarchic interrelation between events in the universe).

This (unexpected) stability and regularity of the hierarchically coupled event-universe is one of the main outputs of our extensive numerical simulation. Here by stability, we understand the relative stability of the dendrogram's structure. The majority of previously happened events preserve their positions. The number of dendrogram's levels is also stable (under appearance of just one new event). By

[2] The treelike geometry was heavily explored in cognitive modelling and psychology [33-38], see even our recent paper on applications of DH-theory to the medical diagnostics of mental disease [39].

[3] Cf. with discrete and fractal approach to quantum physics [40,41].

[4] Although the form of a dendrogram depends on the concrete algorithm, the general structure of theory is the same for all basic algorithms. In our studies, we use the simplest algorithms of 2-adic, 0/1 (yes-no) clusterization.

 doi:10.20944/preprints202204.0193.v1

regularity, we understand the following feature of the dendrogramic dynamics. The branches of a dendrogram can be represented by vectors with 0/1 coordinates or the corresponding natural numbers in the binary representation. At the moment t=k, a dendrogram D_n representing n elementary events has N(D_n)levels. A new elementary event generated at t=k+1 can in principle be any natural number between 0 and 2^{ N(D_n)}. However, this new event can take only very special values (in the natural number representation).

We showed that even random generation of a new event does not induce (statistically) crucial redistribution of events on the dendrogram, the graphs of figures 1, 2 demonstrate some patterns of regularity. As we also see from figure 3, the dendrogramic event-universe is essentially stable w.r.t. appearance of a new event: with high probability most events do not change their tree-representation.

As was noted, the dendrogram dynamics induces not only redistribution of events, but also increasing of dendrogram's size and thus its number of levels. Quite trivially, the number of dendrogram's levels $N= N(D_n)$ for the dendrogram D_n with n events increases with the increase of the number of events n. Similarly, to entropy, $N(D_n)$ can be used to determine *the arrow of time.* However, in contrast to entropy (governed by the second law of thermodynamics, $N(D_n)$ has local minimums on the increasing phone.

The increasing number of levels, which is an expectable feature, is not satisfactory enough to serve as a "thermodynamical" law that concerns only the scale free structure of the dendrogram (in a similar manner we obtained scale free features of dendrograms as the ratio of dendrogramic constants of nature in a recent study [3]). Moreover, we need a macro-state function that, given a certain initial size of a dendrogram, will give us some probabilities on the future macro-state in the dynamical development of the dendrogram or p-adic string representation of the future events. Each of the macro-states will have a finite number of possible micro states. These micro states are all possible dendrogram structures, where n is the number of events. The result of evaluating a certain structural feature of all these micro states will correspond to the same macro state value which is event related . This kind of a state function, like entropy, will provide predictive tools for the dendrogramic dynamics of any developing system of events. To capture the scale free dynamical features of dendrograms dynamics, we use the *shape complexity measure* which was introduced by Barbour et al. in the framework of N-body shape dynamics theory [14-15]. In this context we suggest the following definitions.

1. Definition of a micro state:

Unique dendrogramic structure (coded in a p-adic manner) of relations between events
Or
event's p-adic representation of its relation to the rest of the events

2. Definition of a macro state:

Certain structural feature value that is the same for different dendrogram structures
Or
different p-adic representation of events

Shape Dynamics is a field theory describing gravity differently than General Relativity. Although the differences between the two theories in the most situations are indistinguishable, the two theories have different ontology. Some differences to note are that shape dynamics is not based on spacetime representation; instead, the entities in shape dynamics are three-dimensional geometries fitted together by relational principles. These fitted relations results in *Temporal relationalism* : time emerges from physical changes in shapes. The relational principle of shape dynamics is the Mach-Poincare Principle:

Preprints (www.preprints.org) | NOT PEER-REVIEWED | Posted: 21 April 2022 doi:10.20944/preprints202204.0193.v1

Physical (or relational) initial configurations and their first derivatives alone should determine uniquely the future evolution of the system [15].

This principle is implemented through an intrinsic derivative which is called best matching. The best matching allows one, by using only relational data, to say when points are at the same position at different temporal instances. Moreover, Barbour et al. [10-15] formulated an intrinsic feature of a system serving as physically meaningful labeling of change, where the evolution of the structure of a system is towards configurations (i.e., shapes) that maximize the complexity of the system, in what follows we will define this complexity measure in the event/dendrogramic universe. We note that although previous studies in shape dynamics [9-12] showed that the complexity increase in both directions away from a Janus point and thus determine the arrow of time in symmetrical manner away from a Janus point. However, we cannot produce data in a reverse temporal order and thus cannot find a Janus point with its two opposite symmetrical time arrow directions. Thus, our results will indicate an arrow of time directed from past to future only.

We show in section 5 that the *shape complexity measure* can be used as a statistical law of the dynamics of the evolving dendrograms. This statistical law eventually leads to the determination of the arrow of time in a manner similar to the second law of thermodynamics but with different consequences, which will be discussed in section 7, then when operating with entropy [10, 14-15] .

Our main motivation in this paper is to have the methods and tools to predict behavour of complex systems. In particular, in the framework of medical diagnosis and as a follow up to our recent study on EEG signals of the brain these tools will help us to enticipate epileptic and psychotic seizures [39]

The next two sections are devoted to the brief representation of the foundations of DH-theory. In principle, the reader can jump directly to section 4 in that we consider the (numerically simulated) dendrogramic dynamics for the simplest physical dynamics given by a randomly generated time series. The latter is transferred into the time series of dendrograms. And we study its statistical properties.

2. Brief introduction to epistemic DH-theory

2.1. Info-physical principles

Here we briefly recall the basic principles of DH-theory [1-3]. This theory is about the special information representation physical universe, the event representation (cf. Smolin, Barbour, Rovelli [5-9]).

Principles:

(P1) *Event physics.* The basic structures in nature are events.
(P2) *Relational structures.* Interrelations between events are basic structures of the theory..
(P3) *Hierarchy.* Relational structures are hierarchic.
(P4) *Operational representation.* An observable A is composition of preparation and measurement procedures, P and M: $A= MP$ (first preparation and then measurement).
(P5) *Event-picture of experimental data.* Experimental data is used to form the event-picture. Elementary events are single datapoints; events are subsets of experimental dataset.
(P4) *Relational observables.* Data collected for a physical observable A serves as the input for algorithm Λ for detection of a relational structure. The composition $R= \Lambda A(=\Lambda MP)$ is a *relational observable.*[5]
(P5) *Free will.* The assumption on observer's free will to select different observables (e.g., axes of PBSs) is extended and an observer O has free will to select an event-relational structure expressed via algorithm Λ.

2.2. Mathematical formalism

[5] First preparation, then measurement, and finally clustering algorithm.

Preprints (www.preprints.org) | NOT PEER-REVIEWED | Posted: 21 April 2022 doi:10.20944/preprints202204.0193.v1

We list the main mathematical methods serving as the base of the DH-theory [1-3].
(M1) *Hierarchic clustering algorithms.* Relational structures are determined by hierarchic clustering algorithms.
(M2) *Dendrogramic (treelike) representation.* Outputs of relational observables are dendrograms (finite trees). Dendrograms represent events, their branches (points on the dendrogram's basement) represent elementary events corresponding to measurement's outcomes.
(M3) *Ultrametricity.* Natural metric on a dendrogram is ultrametric based on the common root of two branches, connecting the tree's root with points of the basement of a dendrogram.
(M4) *P-adic number encoding of elementary events.* Elementary events can be encoded by natural numbers and the ultrametric is given by the p-adic absolute value (see Appendix A).

For a big dataset, the set of all subsets is too big. To make the situation numerically treatable, our modelling is restricted to time series, and, for each natural number L, observer O can split the series into blocks of the length L. These are L-events. Denote this event-selection operation by the symbol $\Phi = \Phi(L)$. Model is restricted to relational observables of the form $R = \Lambda\, \Phi\, M\, P$. Consider now clustering algorithm $\Lambda = \Lambda(p)$ with p-branching structure, where $p>1$ is a natural number.

P-adic tree is a homogeneous tree such that, for each node, there are one incoming and p outcoming wedges. P-adic tree with n-levels (branches of length n) is denoted by the symbol $Z(p,n)$. Its branches are encoded either by vectors $x=(x0\ x1\ \dots\ x(n-1)),\ xj=0,\dots,\ p-1$, or by natural numbers $\{0,\ 1,\dots,\ p^{n-1}\}$. In the latter representation, $Z(p,n)$ has the ring structure with *mod* p^n addition, subtraction, and multiplication (see Appendix A).

(M5) *Configuration space.* Relational observable $R=\Lambda(p)\ \Phi(L)\ M\ P$ takes values in $Z(p,n)$, where $n=L-1$.

2.3. Explanatory comments

(C1) *Causal vs. relational structures.* Typically, causal structures are employed as event-relational structures. But this leads to the *apotheosis of the role of space-time* (or at least time, as in works of Smolin, Barbour, Rovelli [5-10]). The use of space-time and causal structures based on it led to tremendous success in natural science. However, events can be related not only via causality, but via more complex relational structures. Moreover, one of the most important physical theories, quantum mechanics, is acausal, at least in some basic interpretations.[6]

(C3) *Bohr's principle of complementarity and event-physics.* Bohr repeatably stated that outcomes of physical observables are not objective properties of systems but generated in the process of a measurement. This is the basic part of his principle of complementarity []. But the notion of a system without objective properties is not so foundationally attractive as the notion explored in classical physics. This led to attempts to define systems operationally via measurement outputs.[7]

(C4) *Operational approach to observation.* This approach is widely explored in quantum measurement theory. It is closely related to the Copenhagen viewpoint that quantum mechanics is about state preparation and measurement procedures, P and M, and outputs of the latter. (In particular, originally the Feynman's integral formalism was rejected by Bohr as unphysical, since it handles system's trajectories between P and M.) However, most operational researchers still refer to systems.

[6] Here we do not discuss "quantum nonlocality", but measurement acausality which was emphasized by von Neumann. This issue is related to solution of measurement problem in quantum mechanics and to theories with hidden variables.
[7] In private discussions with one of the authors (AKH), Zeilinger defined photon as photodetector's click. It is even more natural to consider this click not as the exhibition of the physical system's existence (in this case, photon), but as an event.

Preprints (www.preprints.org) | NOT PEER-REVIEWED | Posted: 21 April 2022 doi:10.20944/preprints202204.0193.v1

(C5) *Real vs. ultrametric representations.* Traditionally, the event-approach to physics has been handled within *real-number representation* with emphasizing the role of space time and causal structure on it (e.g., Smolin, Barbour, Rovelli). Geometrically this is straight-line (multi-dimensional) picture of the universe. However, generally hierarchic relational structures have the treelike geometry. This leads to ultrametric representation. One of the simplest and at the same time well-developed of them is based on *p*-adic trees. We remark that if p=1, then the p-adic tree trivializes and coincides with discretized real line – lattice.

(C6) *Free will vs. total determinism.* In DH-theory, the hypothesis that an observer *O* has free will plays the important role. In physics, free will is treated restrictively as the ability of *O* to select settings of measurement devices, e.g., in the Bell type experiments. In the absence of free will the selection of experimental settings would be predetermined. The latter situation is well accommodated under the superdeterminism hypothesis. Although most quantum physicists accept the free will assumption, others do not. Typically, free will vs superdeterminism are considered as mutually exclusive foundational viewpoints. In DH-theory these view points can be brought closer together as superdeterminism exist as a dynamical law that connects one event to the other (see the action principle in [1,3]) while free of will exist along it side with the choice or rather "the willingness" of how much events the observer decides to observe and how he separate these events into different sub-systems of his observable Universe [2]. Thus in every choice the observer makes his observable universe will still be superdetrmined by the dynamical law.

(C7) *Dimensionality of configuration space.* In physics configuration spaces are multidimensional and the dimension by itself carries physical meaning. In DH-theory, all configuration spaces are treelike, they can be visualized in the Euclidean space as two dimensional structures. Moreover, in general topology their dimension can be characterized internally, and it equals to zero. Hence, we work with *zero-dimensional configuration topological spaces.* This possibility to describe events happening in the four dimensional physical space with the zero dimensional topological structures is the essence of the holographic representation which is basic in DH-theory. Such holography is very special (see [1] for details and illustration by a figure).

3. Brief introduction to ontic DH-theory

In this paper, we work solely with the experimental data

3.1. Principles

(PO1) *Events and relations.* Event-relational hierarchic structure of the universe is mathematically represented by an *infinite tree* endowed with common root ultrametric. Elementary events are represented by branches of the tree; events are all possible sets of branches.

(PO1a) *P-adic universe.* Restriction of trees to p-adic ones gives the p-adic picture of universe: infinite homogeneous tree with one incoming and p-outcoming wedges for each node. This tree is endowed with the ring algebra, addition, subtraction, and multiplication of branches, the ring of p-adic integers $\boldsymbol{Zp}$.

([8]PO2) *Super-determinism.* All possible events are predetermined and simultaneously present in the treelike event-universe.

3.2. Mathematical features of p-adic universe

[8] So, observer's free will disappears in the ontic universe: One may say that "epistemic free will" is apparent; this is observer's illusion generated by incomplete knowledge about the event interrelations. An observer *O* cannot see the complete picture given by the infinite tree of interrelations between events and he has the feeling of free will. But, since *O* would never be able to approach the ontic picture – to map all possible events (in past and future) onto the infinite tree, - for him super-determinism is a theoretical abstraction.

Preprints (www.preprints.org) | NOT PEER-REVIEWED | Posted: 21 April 2022 doi:10.20944/preprints202204.0193.v1

(U1) ***Zp*** is totally disconnected.[9]
(U2) ***Zp*** is disordered: it is impossible to introduce an order structure compatible with algebraic operations.
(U3) ***Zp*** is zero dimensional as a topological space.

4. predictability of evolving dendrogram

We started by examining n events ($E_m \; where \; m \in 1,2 \dots n \;\; and \; n = number \; of \; events$), for that purpose we generated n random numbers (in the figures below we show the example for n=50, but examining different n's was done with the same qualitative results). From these base n events we constructed a dendrogram D_n by using the procedure outlined in appendix B. We then add another event generated randomly and from the n+1 events we compose a dendrogram D_{n+1}.

Thus for the dendrogram D_n we have n branches each path of branch m

$$where \; m \in 1,2 \dots n \;\; and \; n = number \; of \; events$$

from root to leaf corresponds to event m. each branch is a string of 1/0 where 1 represents bifurcation of the branch to the left and 0 is a bifurcation of the branch to the right. This string can be represented by a natural number V_m by using the the p-adic expansion

$$V_m = \sum_{i=1}^{k} a_i 2^{i-1} \;\; where \; a_i \in 0,1 \; and \; k = maximal \; ball \; of \; dendrogram$$

Thus we represent each event as a natural number which corresponds to the event path in the dendrogram.

Our main concern is to understand to what extend we can predict what will be the natural number V_{m+1} representing event E_{n+1} in the D_{n+1} dendrogram. For that purpose, we followed the following procedure:

1. We randomly generated a base (fixed) n events and composed out of it the n edges dendrogram
2. Then to the same n events we added one more event $E_{n+1}$and computed its natural number representation V_{n+1}.
3. We generated the E_{n+1} event 6000 times and each time computed its V_{n+1}.
4. We then changed the base n events and repeated steps 2 and 3 for this new n base events
5. We changed the base n events 100 times

We first checked what will be V_{n+1} (the p-adic expansion representing E_{n+1}) in the following case: E_{n+1} doesn't cause the original dendrogram D_n (with 50 edges) to change the number of levels in it. So, if, for example, D_n has 9 levels, D_{n+1} has 9 levels as well. As is shown in figure 1, the natural number V_{n+1} representing $E_{n+1}$is very predictable and tends to favour values closer to

$$2^k - 1 \; where \; k \in -\inf, 1 \, , 2 \dots r \;\; and \; r = \max ball \; of \; dendrogram$$

in each interval [2^k_i 2^k_{i+1}]. We also see that less than 400 natural numbers were obtained out of 512 possible such numbers

[9] The formal topological definition [33] is that each point *x* has the basis of neighbourhoods which are at the same time open and closed ("clopen"). It is equivalent to more intuitive definition. the set of locally constant functions (i.e., constructed from characteristic functions of balls) is dense in the space of real-valued continuous functions. Another interesting property is that any continuous trajectory t to x(t) with real time parameter t is piecewise constant; so the real time dynamics consists of jumps.

Preprints (www.preprints.org) | NOT PEER-REVIEWED | Posted: 21 April 2022 doi:10.20944/preprints202204.0193.v1

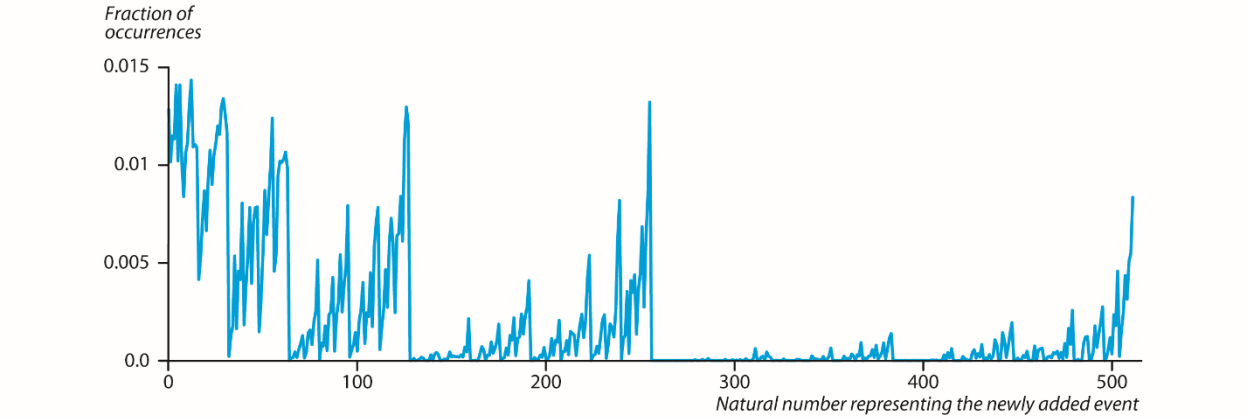

Figure 1 probability density function of natural number representing the p-adic expansion representing an added event. We generated base 50 random numbers and added 6000 times another random number (E_{n+1}) to them resulting in 51 edges dendrogram . adding the extra event was done under the restriction that D_n and D_{n+1} both had number of levels equal to 9. we repeated the procedure for 100 base 50 random numbers. For all 100 base 50 random numbers we show the distribution of the possible value of the natural number V_{n+1} representing E_{n+1}. About 400 such natural number values occurred out of 512.

We also show (in figure 2) that given one fixed base 50 events only very limited set of natural numbers can result which represents the E_{n+1} event: around 80 such natural numbers out of possible 512 (9 levels of dendrogram). Although in figures 1,2, we simulated with $n = 50$ base events dendrograms where D_n and D_{n+1} both had number of levels equal to 9, we witnessed similar qualitative results with 100,150,200…500 base events and different number of levels.

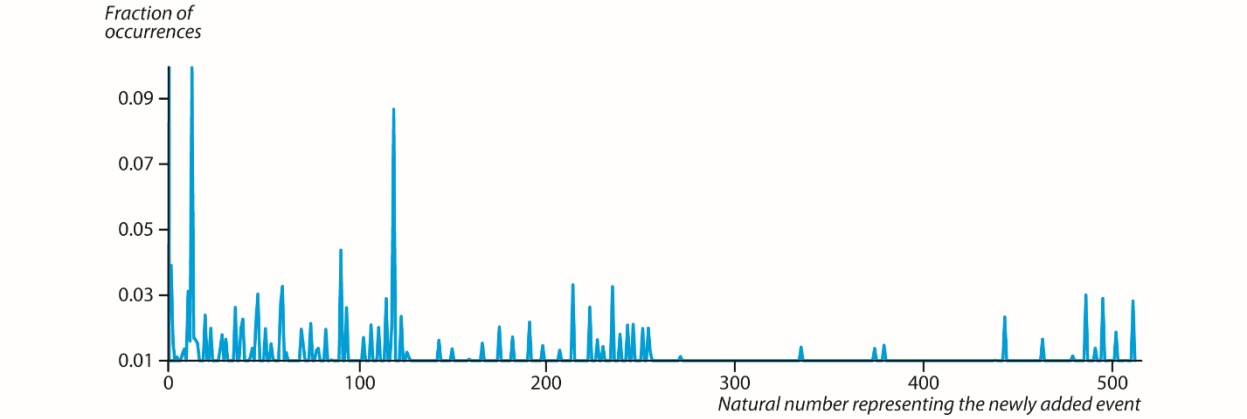

Figure 2 probability density function of natural number representing the p-adic expansion representing an added event. We generated only oned base 50 random numbers and added 600000 times another random number (E_{n+1}) to them resulting in 51 edges dendrogram . we show the distribution of the possible value of the natural number V_{n+1} representing E_{n+1}. About 80 such natural number values occurred out of 512.

Moreover, we checked how many V_m in the D_n dendrogram will change their natural number representation upon adding the E_{n+1} event with the result of a D_{n+1} dendrogram. This is shown in figure 3 which demonstrated essential stability of the dendrogram representing n events w.r.t. to appearance of a new event.

Preprints (www.preprints.org) | NOT PEER-REVIEWED | Posted: 21 April 2022 doi:10.20944/preprints202204.0193.v1

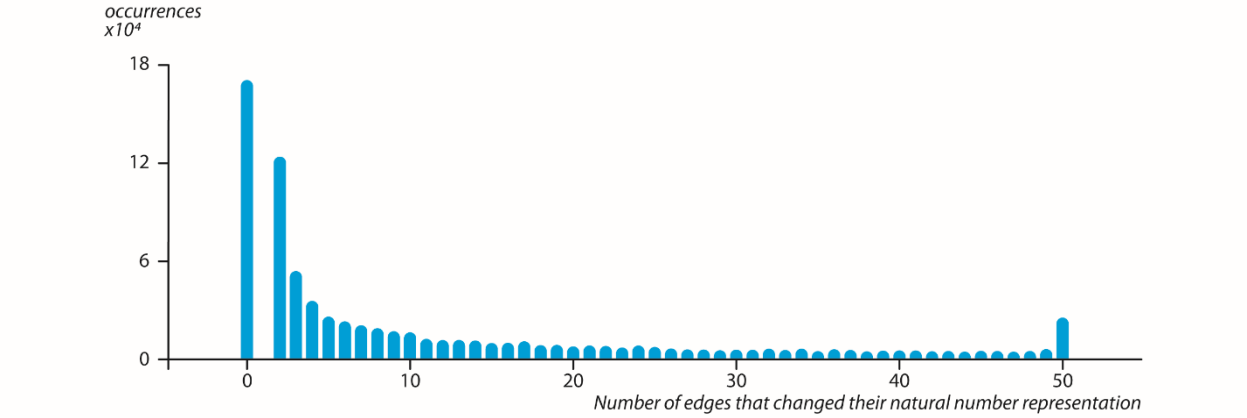

Figure3 possible rearrangements of dendrogram structure upon adding a new event. We generated only oned base 50 random numbers events $E_1 - E_{50}$ and added 600000 times another random number (E_{n+1}) to them resulting in 51 edges dendrogram. adding the extra event with the restriction that D_n and D_{n+1} both had number of levels equal to 9. We checked, for each iteration, how many of the base 50 events p-adic representation changed upon adding the extra event E_{51}

Furthermore, when we removed the restriction that if $N(D_n)$=9 then N(D_{n+1})=9 . Thus in the case where $N(D_n)$=9 but N(D_{n+1}) can have any maximal ball value by adding E_{n+1} we again witnessed the same qualitative results as in figure 1 but with more possible V_m values (figure 4)

Figure 4

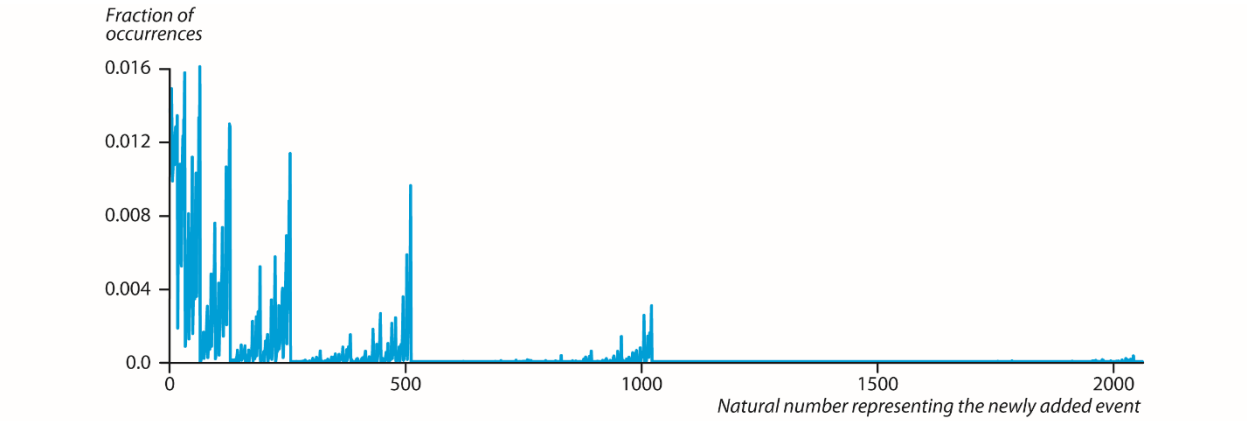

Figure 4 probability density function of natural number representing the p-adic expansion representing an added event. We generated base 50 random numbers and added 6000 times another random number (E_{n+1}) to them resulting in 51 edges dendrogram . adding the extra event without the restriction that D_n and D_{n+1} both had number of levels equal to 9. we repeated the procedure for 100 base 50 random

Preprints (www.preprints.org) | NOT PEER-REVIEWED | Posted: 21 April 2022 doi:10.20944/preprints202204.0193.v1

numbers. For all 100 base 50 random numbers we show the distribution of the possible value of the natural number V_{n+1} representing E_{n+1}. About 400 such natural number values occurred out of 512.

Again checking how many edges in the D_n dendrogram will change their natural number representation upon adding the E_{n+1}.with the result of a D_{n+1} dendrogram. We see (figure 5) that although now D_{n+1} can result in any maximal ball value we obtain the same qualitative result as in figure 3 which is with the restriction that if the $N(D_n) = 9$ then $N(D_{n+1}) = 9$.

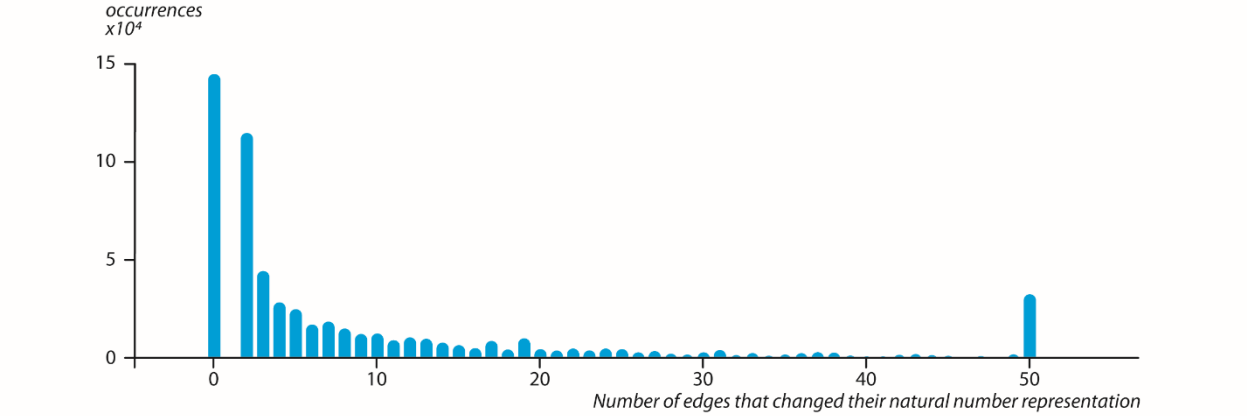

Figure 5 possible rearrangements of dendrogram structure upon adding a new event. We generated only oned base 50 random numbers events $E_1 - E_{50}$ and added 600000 times another random number (E_{n+1}) to them resulting in 51 edges dendrogram. adding the extra event without the restriction that D_n and D_{n+1} both had number of levels equal to 9. We checked, for each iteration, how many of the base 50 events p-adic representation changed upon adding the extra event E_{51}

Checking the number of levels of the newly formed dendrogram D_{n+1} showed a very significant peak in the maximal ball value of 9 (figure 6)

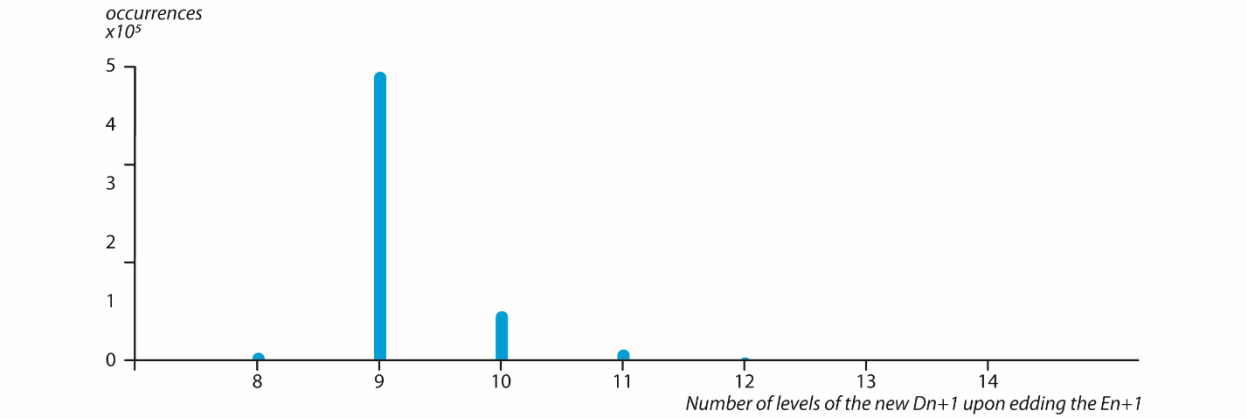

Figure 6 Number of levels of the new D_{n+1}upon edding the E_{n+1} . We generated only oned base 50 random numbers events $E_1 - E_{50}$ and added 600000 times another random number (E_{n+1}) to them resulting in 51 edges dendrogram. adding the extra event without the restriction that D_n and D_{n+1} both had number of levels equal to 9. We checked, for each iteration, what will be $N(D_{51})$ when $N(D_{50}) = 9$

Preprints (www.preprints.org) | NOT PEER-REVIEWED | Posted: 21 April 2022 doi:10.20944/preprints202204.0193.v1

5. Complexity measures of events and dendrograms

Our main motivation in this section is to understand the dynamical process which changes the dendrogram structure upon adding more and more events. In order to obtain a meaningful measure of dendrogramic structure dynamics, we need to overcome the trivial problem that by adding events to a dendrogram we are repeatedly making the dendrogram larger. So, we have a sequence D_n , D_{n+1} , D_{n+2} …. .We therefore need some scale invariant measure of the system.

Interestingly we have shown in previous study [???] the scale free similarities between different size dendrogram and their relations to the constants of nature $G, h \; and \; c$. In order to quantify in a scale free manner, the complexity of a dendrogram structure (and even the structure of a single branch in a dendrogram, as detailed below), we decided to use the complexity measure suggested by Julian Barbour in his studies of N-body shape dynamics.

We first present Barbours complexity measure in an N-body system with N masses

$$l_{rms} = \frac{\sqrt[2]{\sum_{i=1}^{N-1}\sum_{j=i+1}^{N} m_i m_j r_{ij}^2}}{M} \quad and \quad \frac{1}{l_{mhl}} = \frac{1}{M^2}\left(\sum_{i=1}^{N-1}\sum_{j=i+1}^{N}\frac{m_i m_j}{r_{ij}}\right)$$

$$shape\ complexity\ measure = \frac{l_{rms}}{l_{mhl}}$$

5.1. Complexity measure of dendrograms.

We started from n=50 events (random numbers) that were composed into dendrogram than we added one event at a time and composed the dendrogram of n+1 events. This procedure was done repeatadly up until the event n=5000. In order, to measure the shape complexity of the dendrogram , with n events , we assign

$m_i = V_i \;\; where \; V_i$ is the monna map representing the i′th dendrogram branch p − adic expansion

$$V_i = \sum_{m=1}^{k} a_m 2^{-m-1} \;\; where \; a_m \in 0{,}1 \; and \; k = maximal\ ball\ of\ dendrogram$$

And

$$r_{ij} = |V_i - V_j| \; where \; i < j$$

By adding more and more events the dendrogram shape complexity measure tends to rise. The mean of the distribution of the shape complexity measure values constantly move its peak to higher values (figure 7)

Preprints (www.preprints.org) | NOT PEER-REVIEWED | Posted: 21 April 2022 doi:10.20944/preprints202204.0193.v1

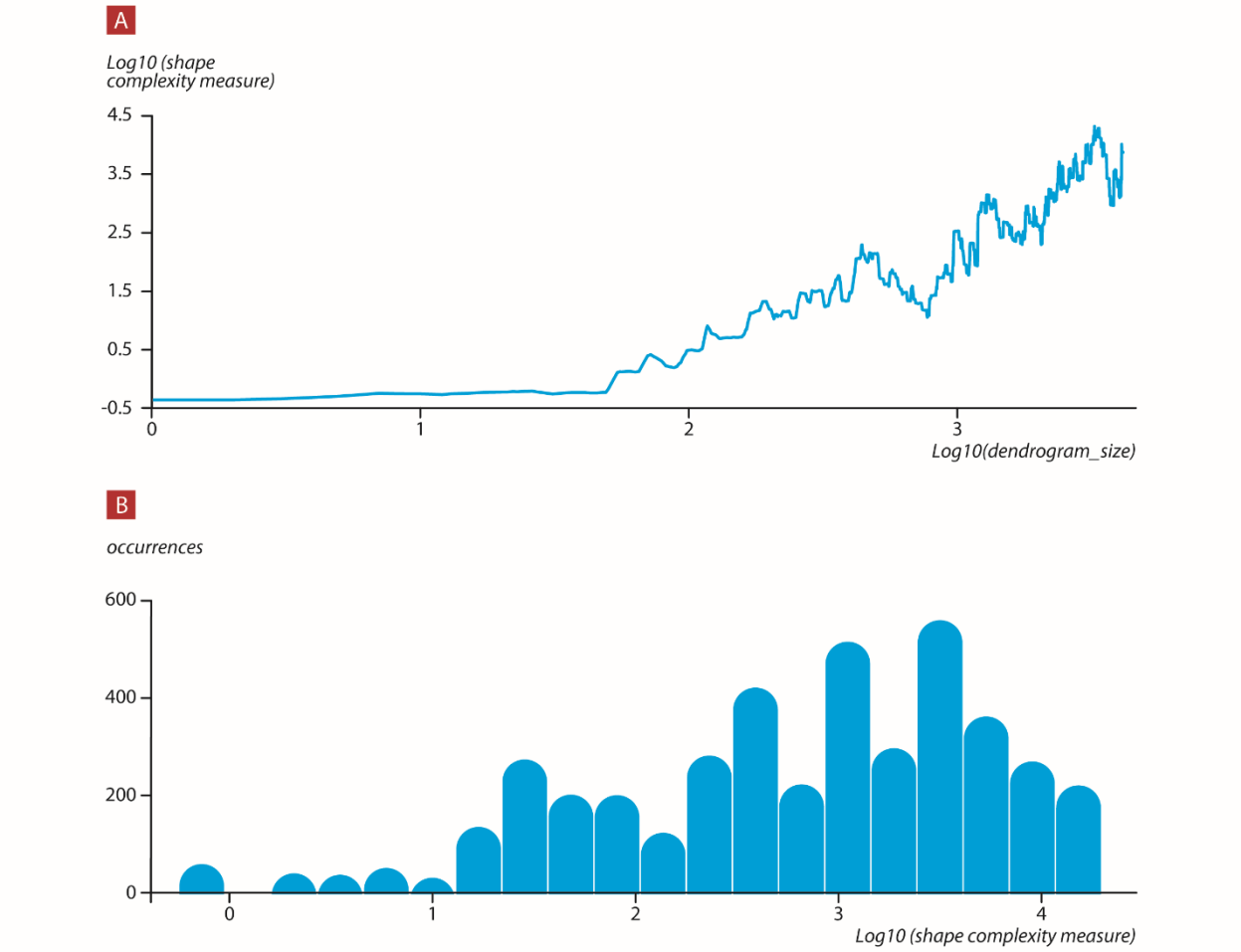

Figure 7 shape complexity measure of dynamically growing dendrograms. **A**. We started with only one base 50 random numbers events $E_1 - E_{50}$ and added each time an extra event E_n where n=51,52…5000 resulting in a dendrogram sequence $D_{50}, D_{51} \ldots . D_{5000}$ for each such dendrogram we computed its shape complexity measure. **B**. histogram of the shape complexity measure values of the 4950 dendrogram structures.

5.2. **Complexity measure of the ball distribution in the p-adic representation of an event**

We again started from n=50 events (random numbers) that were composed into dendrogram than we added one event at a time and composed the dendrogram of n+1 events. This procedure was done repeatadly up until the event n=5000. Each time we examined the added event, the n+1 event, branch 1/0 string and then we calculate the shape complexity measure in the following way: for a string $a_1, a_2, a_3 \ldots . a_n$ we identify the $i \; where \; a_i = 1$ this is a p-adic ball value

thus

$$m_j = i \; where \; a_i = 1$$

And

$$r_{kj} = |m_k - m_j|$$

Preprints (www.preprints.org) | NOT PEER-REVIEWED | Posted: 21 April 2022 doi:10.20944/preprints202204.0193.v1

Again by adding more and more events the next event branch string shape complexity measure tends to rise. The mean of the distribution of the shape complexity measure values constantly tend to move its peak to higher values (figure 8).

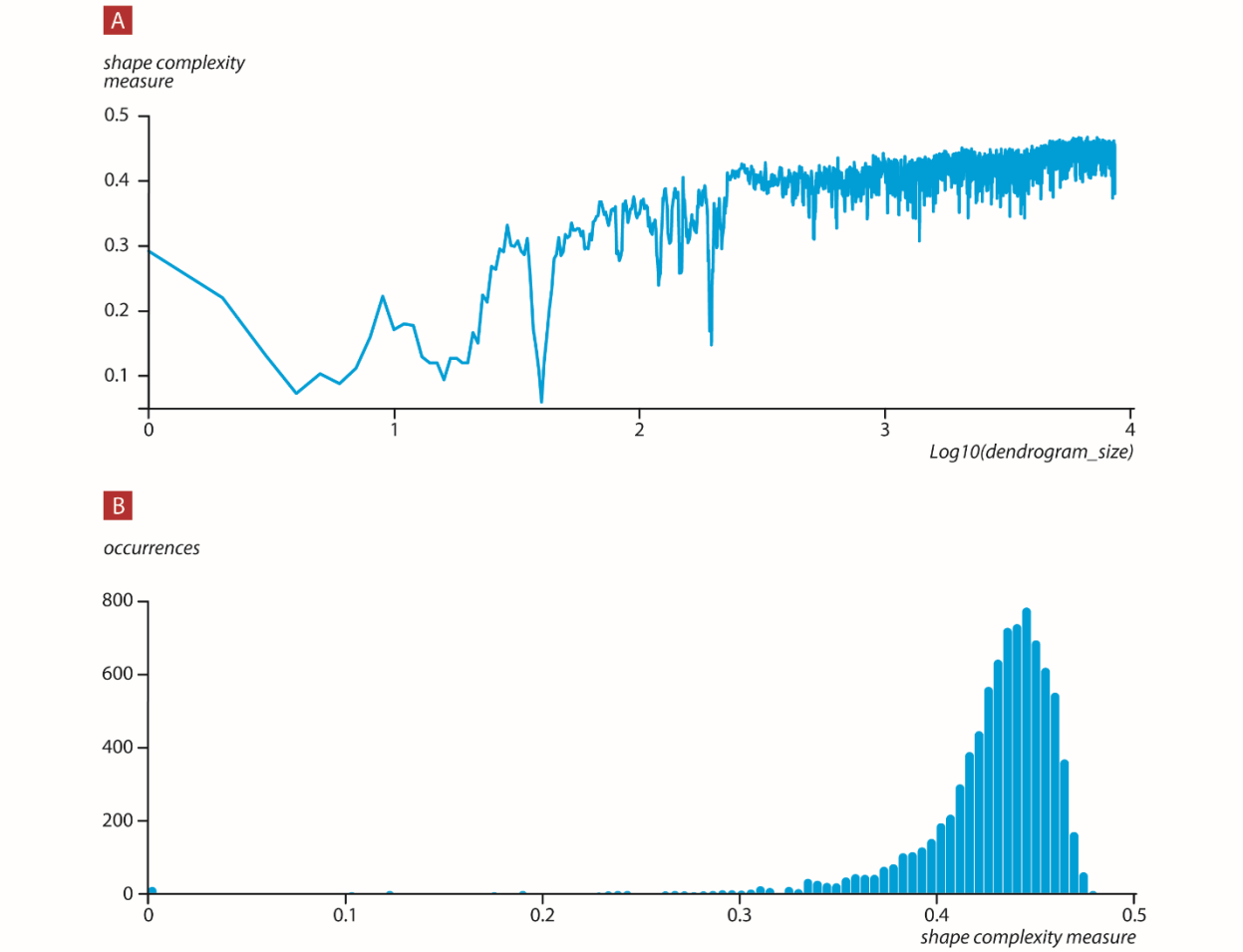

Figure 8 shape complexity measure of p-adic representation of the next added event . **A**. We started with only one base 50 random numbers events $E_1 - E_{50}$ and added each time an extra event E_n where n=51,52…5000 resulting in a dendrogram sequence D_{51} …. D_{5000} and a p-adic representation of the added event E_{51} …. E_{5000} for each such event we computed the shape complexity measure of its p-adic representation in the D_n dendrogram . **B**. histogram of the shape complexity measure values of the p-adic representation of the E_n event in the D_n dendrogram of the 4950 events.

One can argue that these results are trivial as by adding sequentially one event at a time the dendrogram increases in size and the next event branch path is represented by a longer string, thus we move to higher N number of "bodies". In order to show that higher shape complexity values do not depend on possible larger N number of "bodies" in the system, we turn into our static Universe view which was advocated in our recent papers. We generated a temporal sequence of n random number of events and produced, from all n events, their static representative dendrogram where their temporal feature was not included in order to form the dendrogram. We then calculated the 3 body shape complexity measure obtained from the dendrogram in the following way:

Preprints (www.preprints.org) | NOT PEER-REVIEWED | Posted: 21 April 2022 doi:10.20944/preprints202204.0193.v1

We start with the first h temporally events and mark them as the past of the h+1 event. Thus our 3 bodies are the Universal past of the h+1 event which is calculated as follows :

$$\boldsymbol{B} = \sum_{j=1}^{h} V_j \quad where\ V_j\ is\ a\ natural\ number\ such\ that$$

$$V_j = \sum_{m=1}^{k} a_m 2^{m-1} \quad where\ a_m \in 0{,}1\ and\ k = maximal\ ball\ of\ dendrogram$$

We represent B as a binary string b and calcuculate

$$m_{past} = m_1 = \sum_{m=1}^{k} b_m 2^{-m-1} \ where\ b_m \in 0{,}1\ and\ k = length\ of\ binary\ string$$

, the present $m_{present} = m_2 = V_{h+1}$

$where\ V_{h+1}$ is the monna map representing the present (h + 1) dendrogram branch p − adic expansion

$$V_{h+1} = \sum_{m=1}^{k} a_m 2^{-m-1} \quad where\ a_m \in 0{,}1\ and\ k = maximal\ ball\ of\ dendrogram$$

and the center of mass of the present and the past $m_3 = (m_1 - m_2)/2$. We then calculate the above mentioned shape complexity measure for h=50,51…4950 (thus moving the present each time one event to the future).

where

$$r_{kj} = |m_k - m_j|$$

For each such temporal sequence we randomized the temporal order of events 10 times and calculated again the complexity measure the non-temporal ordered sequence.We show the result of the progressing mean values (thus the mean of values of 1 to k where k =100,200…4900) of complexity measures values in figure 10A across all 400 temporal sequences and the progressing mean values of complexity measures values across all 100x400 of randomized temporality sequences and

when we move forward the present one event at a time in the direction of our future produced events we show, in the figure below, that the shape complexity measure grows with time. Upon reversing the direction of time, thus we move the present from the future to the past, our 3 bodies system is composed of the Universal future of the, $where\ the\ number\ of\ events\ in\ the\ future\ is$: $(total\ number\ of\ events) - h,$ event which is calculated as follows:

$$\boldsymbol{B} = \sum_{j=\text{number of events}}^{number\ of\ events-h} V_j \quad where\ V_j\ is\ a\ natural\ number\ such\ that$$

$$V_j = \sum_{m=1}^{k} a_m 2^{m-1} \quad where\ a_m \in 0{,}1\ and\ k = maximal\ ball\ of\ dendrogram$$

We represent B as a binary string b and calcuculate

Preprints (www.preprints.org) | NOT PEER-REVIEWED | Posted: 21 April 2022 doi:10.20944/preprints202204.0193.v1

$$m_{future} = m_1 = \sum_{m=1}^{k} b_m 2^{-m-1} \; where \; b_m \in 0,1 \; and \; k = length \; of \; binary \; string$$

the present is $m_2 = V_{number\ of\ events-h\ -1}$ and calculated as above , and the center of mass obtained from the present and the past is $m_3 = (m_1 - m_2)/2$. we again calculate the above mentioned shape complexity measure for h=50,51…4950 (thus moving the present each time one event to the past)

where

$$r_{kj} = |m_k - m_j|$$

For the randomized temporal order of events we calculated again the complexity measure the non-temporal ordered sequence, now in regards to the present and future as definend above .We show the result of the progressing mean values (thus the mean of values of 1 to k where k =100,200…4900) of complexity measures values in figure(10B) across all 400 temporal sequences and the progressing mean values of complexity measures values across all 100x400 of randomized temporality sequences and

As can be seen in figure 9A-B the shape complexity measure grows always if we consider the present direction from past to future (9 A) in both past-present system and future to past in the future-present system, where we set the positive direction as for present moving from the past towards the future. The real temporal order of the sequances results in the present-past and present-future system complexity measure values to be below the mean of the same systems that are randomized in a non- temporal order

Preprints (www.preprints.org) | NOT PEER-REVIEWED | Posted: 21 April 2022 doi:10.20944/preprints202204.0193.v1

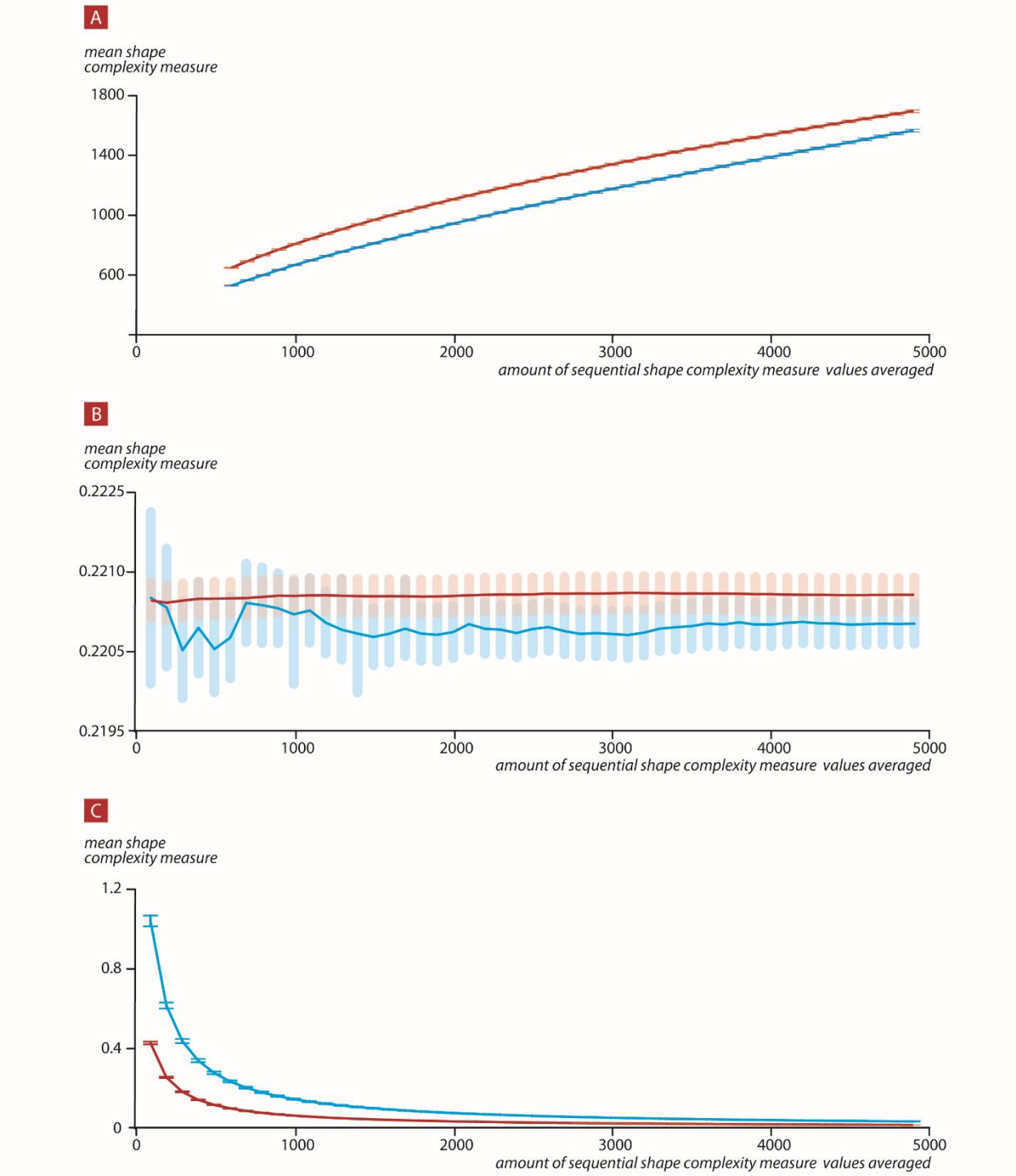

Figure 9 Shape complexity measure of the p-adic representation in the dendrogramic 3-body system. we created for that purpose 400 static dendrograms (each event was created in an increasing temporal manner) each with 5000 events/edges **A** calculating for each sequence the mean complexity measure of its first n values where n=100,200..4900. we show the mean±se of this mean value of across the 400 dendrograms generated in the past-present system when present move in the direction of the future. **B** calculating for each sequence the mean complexity measure of its first n values where n=100,200…4900. we show the mean±se of this mean value across the 400 dendrograms generated in the future-present

Preprints (www.preprints.org) | NOT PEER-REVIEWED | Posted: 21 April 2022 doi:10.20944/preprints202204.0193.v1

system and their mean value when present move in the direction of the future. **C** calculating for each sequence the mean complexity measure of its first n values where n=100,200…4900. we show the mean±se of this mean value across the 400 dendrograms generated in the past-present-future system when present move in the direction of the future.

Again in both simulation, past to future and future to past , we have m_1 increasing in size as a p-adic expansion string. Thus again one can argue that the size of the Universal past\future gets larger which influence the shape complexity measure to go up. Thus we need to overcome the argument that one component's p-adic string (m_1) in the 3 body system gets increasingly bigger. For that purpose we again defined the past, present and future as m_1 and m_2 as outlined above for h=50,51…4950 (thus moving the present each time one event to the future). As can be seen in the figure 10C, the shape complexity decreases when considering the whole system of past, present and future where we set the positive direction as when the present moves from the past towards the future .More over the real temporal order of the sequances results in both systems mean complexity measure values that are above the mean of systems that are randomized in a non- temporal order.

The above complexity measures are clearly rational numbers and as such not p-adic. Thus, we moved from the p-adic 1 bounded ball, where our dendrogram resides in, to the whole of the rational number field. This is an unwanted outcome. In order to overcome this problem we represented each complexity measure rational number as a p-adic expansion string and calculated the string complexity measure as outlined above. In the figure below we show the results of the "p-adic representation of the complexity measure" or as we call it the "double Shape complexity measure"

Preprints (www.preprints.org) | NOT PEER-REVIEWED | Posted: 21 April 2022 doi:10.20944/preprints202204.0193.v1

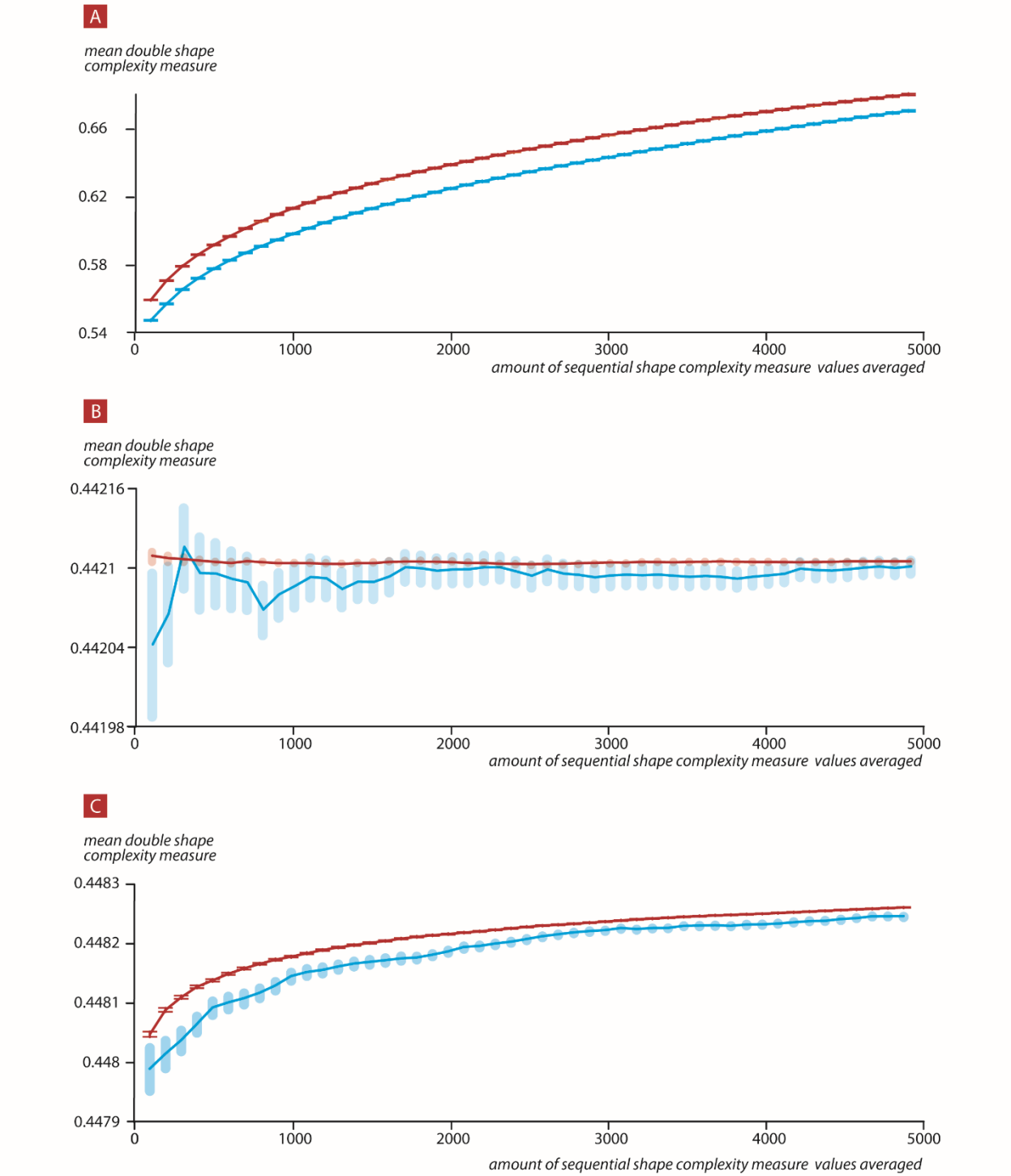

Figure 10 double Shape complexity measure of the p-adic representation in the dendrogramic 3-body system. we created for that purpose 400 static dendrograms (each event was created in an increasing temporal manner) each with 5000 events/edges **A** calculating for each sequence the mean double complexity measure of its first n values where n=100,200..4900. we show the mean±se of this mean value across the 400 dendrograms generated in the past-present system when present move in the direction of the future. **B** calculating for each sequence the mean double complexity measure of its first n values

Preprints (www.preprints.org) | NOT PEER-REVIEWED | Posted: 21 April 2022 doi:10.20944/preprints202204.0193.v1

where n=100,200…4900. we show the mean±se of this mean value across the 400 dendrograms generated in the future-present system when present move in the direction of the future. **C** calculating for each sequence the mean double complexity measure of its first n values where n=100,200…4900. we show the mean±se of this mean value across the 400 dendrograms generated in the past-present-future system when present move in the direction of the future.

Please note that now the whole universe system goes up when the present progress to the future with an asymptote of the p-adic ball of 2 thus to 2^-1. The most interesting feature is revealed in the two top figures namely in the past and present system, where the present moves in the direction of the future, the complexity measure increases from values greater then 2^-1 and approaches to values closer to 2^0 , while in the future and present system, where the present moves in the direction of the future, the complexity measure icreases from values greater then 2^-2 and approaches to values closer to 2^-1. Thus the value 2^-1 or the p-adic 2 ball is the janus point of the two systems. These are two "separate" systems that operate dynamicaly on two different p-adic balls, where in both the time arrow is defined by the complexity measure.

6. P-adic complexity measure of rational numbers

Any rational number can be represented by its a p-adic expansion; thus again we can calculate its complexity measure of balls distribution as outlined above. We generated a 200 series of random numbers in the interval [0 1] . each series contained 5000 such random rational numbers which were created temporaly. For each random number we calculated its complexity measure of balls distribution. For n=100,200…4900 we calculated the mean of the first number to the n's complexity measure values (plot on the left). When we calculated from this rational number its double complexity measure value the double complexity measure of its p-adic expansion showed a reversed picture of temporality (on the right)

Preprints (www.preprints.org) | NOT PEER-REVIEWED | Posted: 21 April 2022 doi:10.20944/preprints202204.0193.v1

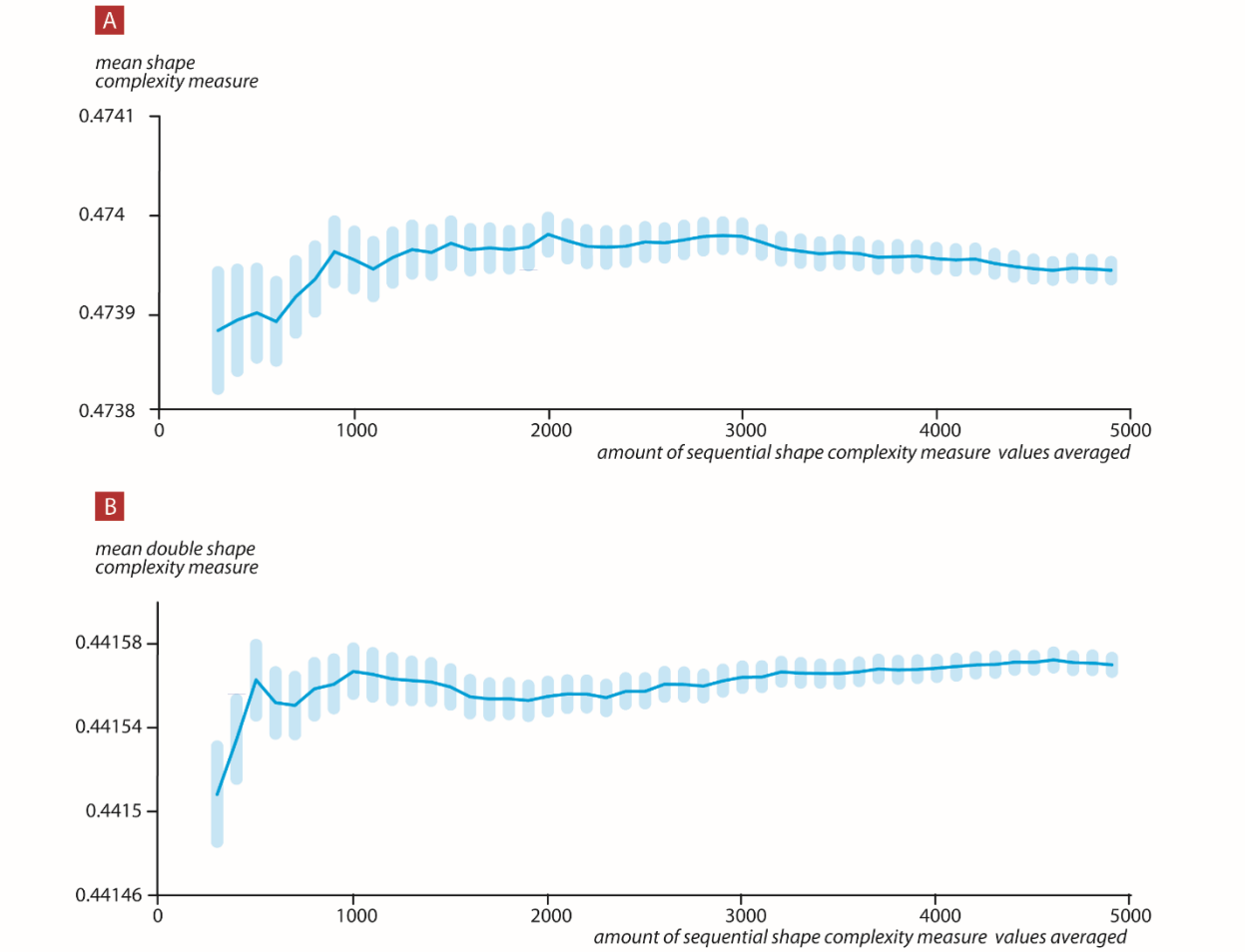

Figure 11 Shape complexity measure of the p-adic representation of a random number . we created for that purpose 800 temporal sequences (each event/random number was created in an increasing temporal manner) of 5000 random numbers we then calculated for each number in each sequence its p-adic representation Shape complexity measure. **A** we then calculated for each sequence the mean complexity measure of its first n values where n=300,400,4900. we show the mean±se across the 800 sequences. **B** we the calculated for each sequence the mean double complexity measure of its first n values where n=300,400,4900. we show the mean±se of this mean value of across the 800 sequences

Concluding remarks

DH-theory was created as the novel mathematical representation of natural phenomena which is an alternative to the standard space-time picture. Similarly, to, e.g. Smolin, Barbour, Rovelli [5-14], the universe is composed of events, so we work in the event-universe. In DH-theory elementary events are represented by branches of dendrograms (finite trees). We start the paper with formalization of DH-theory, by listing and commenting its basic structures and briefly presenting its mathematical basis.

The main part of this paper is devoted to study of dynamics of the event-universe generated by appearance of new events. We found (via extensive numerical simulation) that surprisingly the dendrogramic space structure is relatively stable. In principle, generation of new event can lead to total recombination of dendrogram's branches. However, this is not the case (see histograms at figures of section 4). Even randomly generated events are concentrated at the special sectors of the natural number

Preprints (www.preprints.org) | NOT PEER-REVIEWED | Posted: 21 April 2022 doi:10.20944/preprints202204.0193.v1

representation of events (branches) and with high probability the rest of the dendrogram is only slightly modified or even stable. We can say that dendrogramic universe evolves towards a few special sectors and this specific evolution is not a consequence of special dynamical laws, but of the treelike structure of the event universe.

We show that given some initial data we can predict the future macro state of the system where this macro state corresponds to a complexity measure value that was first suggested by Barbour and here implemented on dendrograms and p-adic expansion strings. We note again that the ideology and principles of DH-theory are closely related to Shape dynamics (and in fact were inspired by some of the theory's ideas). The complexity scale free measure implemented on p-adic field defines the time arrow and combined with the dendrogram size and natural numbers probability densities can be used to predict the dynamical evolution of dendrograms as well as any random number generated sequence. Moreover we found that the two systems (past-present and present-future) follow the same time arrow, from past to future. The double p-adic complexity measure, demonstrates that these two systems operate in two distinct ranges of the p-adic field where opposite time directions move away from the 2^{-1} value. This result is in good agreement with Barbour et al. studies of 3 body shape dynamics simulations. Thus overall the complexity of a system, even if randomly generated, increases. This in turn elevates problems with the entropic law where increasing disorder, which is in contradiction to the state of the universe, is always expected. We hope that these tools can be implemented in real systems that produce non-random signal in order to predict their dynamics (in particular biological signals from EEG signals for prediction of unwanted events and condition [39])

DH-theory can be applied to model not only the physical, but even to biological evolution. Our result supports evolution theory in which the variety of new possible evolutionary events is constrained by the hierarchic relational (treelike) structure of previously happened events. But, this is the topic for a separate work.

Acknowledgments: Varda and Boaz Dotan, Hirsha Leib Tsofnat and Abraham Shor

Appendix A. Ultrametric Spaces, Trees, p-Adic Numbers

I

In this appendix, we follow the non-expert friendly presentation from paper [3]. In some applications, the point structure of a set X and the properties of a metric ρ may essentially differ from the Euclidean case. We are interested in metric spaces X where, instead of the standard triangle inequality, the strong triangle inequality,

$$\rho(x, y) \leq max[\rho(x, z), \rho(z, y)] \quad \text{(A1)}$$

is valid. Such a metric is called an ultrametric, and such metric spaces are called ultrametric spaces. The strong triangle inequality can be stated geometrically: all triangles are isosceles.

Let us discuss the main properties of ultrametric space X. We set

$$B_r(a) = \{x \in X: \rho(x - a) < r\}, B_r \sim (a) = \{x \in X: \rho(x - a) \leq r\}, r > 0, a \in X \quad \text{(A2)}$$

These are balls of the radius r with the center at the point a. Our standard intuition tells us that $B_r(a)$ is a closed ball, but not open, and $B_r \sim (a)$ is an open ball, but not closed. However, it is not valid for ultrametric spaces.

In an ultrametric space, each ball in X is open and closed at the same time. Each point of a ball may serve as a center. A ball may have infinite radii.

Preprints (www.preprints.org) | NOT PEER-REVIEWED | Posted: 21 April 2022 doi:10.20944/preprints202204.0193.v1

Let U and V be two balls in ultrametric space X. Thus, there are only two possibilities: (1) the balls are ordered by inclusion (i.e., $U \subset V$ or $V \subset U$); (2) the balls are disjointed.

Thus, if two balls have a common point, then one has to be a part of another.

The symbol $S_r(a)$ denotes the sphere $\{x \in X: \rho(x, a) = r\}$ of the radius $r > 0$ with the center at a. There is also a large deviation from the Euclidean case; the sphere $S_r(a)$ is not a boundary of $B_r(a)$ or $B_r \sim (a)$.

Consider the following class of ultrametric spaces (X, ρ). Every point x has an infinite number of coordinates

$$x = (a_o, a_1, ..., a_n)\ldots).$$

Each coordinate yields a finite number of values $a \in \{0, ..., p - 1\}$, where $p > 1$ is a natural number. We denote the space of sequences (1) by the symbol $X = \mathbf{Zp}$. The standard ultrametric is introduced in this set in the following way.

Let $x = (a_0, a_1, a_2, ..., a_n)$, $y = (b_0, b_1, b_2, ..., b_n) \in \mathbf{Zp}$. We set

$$r\_p\ (x, y) = 1/p^k \qquad \text{if } a_j = b_j,\ j = 0, 1, ..., k - 1, \text{ and } a_k \neq b_k \tag{A3}$$

This is a metric and even an ultrametric. To find the distance $r\_p(x, y)$ between two strings of digits, x and y, we have to find the first position k at which the strings have different digits. The space $X = \mathbf{Zp}$ coincides with the unit ball centered at zero, $X = B_1(0)$; this space is compact. Geometrically, it can be represented by the tree (see Figure A1 for the 2-adic tree representing **Z2**). Here, one vertex, the root labeled as R, is incidental for two edges and other vertices are incidental for three edges. We noticed that it is convenient to consider this tree as the directed graph; for each vertex I different from R, one edge comes from the branch starting at R, the "input edge", and two edges go out from I, the "output edges". These two edges (or vertices at their ends) are labeled by $a = 0, 1$. In **Figure A1**, the order of labeling of the output edges is based on the embedding of the tree in the plane, the upper output edges are labeled by 0 and the lower by 1. This leads to the concrete numerical representation of this tree. However, the rule used for the labeling of edges is not obligatory; for each vertex I, we can assign 0/1 to each of the output edges in an arbitrary way and obtain another numerical representation of this tree.

Any finite string, $x = (a_o, a_1, ..., a_n)$, $a_j = 0,1,.., p-1$, can be represented by the natural number which w.r.t. powers of p, p-adic expansion, is given by this string; in particular, if p=2, then this is the usual binary expansion of the natural number. Thus the set of natural numbers $\boldsymbol{N}$ is embedded into $\boldsymbol{Zp}$ for each p >1. An infinite string, $x = (a_o, a_1, ..., a_n\ldots)$, $a_j = 0,1,.., p-1$, is represented by the power series converging w.r.t. the p-adic ultrametric. On the set of these series, one can define the operations of addition, subtraction, multiplication; they are obtained as extensions by continuity of the corresponding operations on natural numbers. (The set of natural numbers $\boldsymbol{N}$ is dense in $\boldsymbol{Zp}$). In this paper, we considered only finite trees, i.e., their branches are encoded by finite strings of 0/1 (the 2-adic clustering algorithm was used). Thus we can operate on the set of natural numbers $\boldsymbol{N}$ endowed with the ultrametric induced from $\boldsymbol{Zp}$.

Preprints (www.preprints.org) | NOT PEER-REVIEWED | Posted: 21 April 2022 doi:10.20944/preprints202204.0193.v1

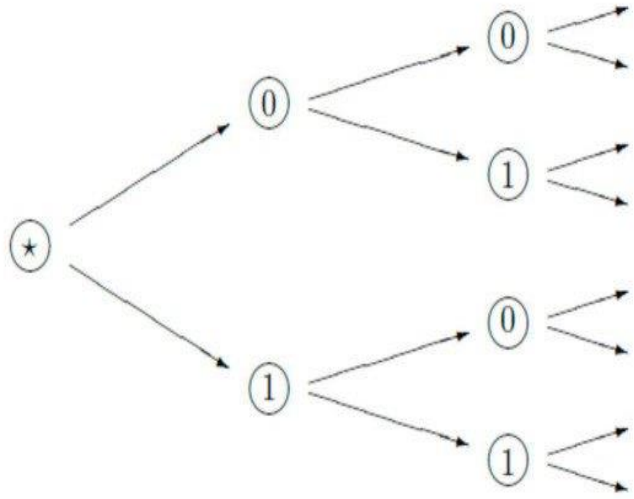

Figure A1: 2-adic tree, geometric image of **Z2.**

Appendix B.

Step 1. Producing an agglomerative hierarchical cluster binary tree from a temporal sequence of random number.

Step 1.1

Calculating the pairwise distance matrix: for a single $Event_j, where\ j \in$ 1,2..$N\ N = number\ of\ random\ numbers\ produced\ in\ temporal\ sequence$.

We then calculated $\|Event_i - Event_j\|$ where $\|\ \|$ is the Euclidean distance between the i'th event and j'th event.

Step 1.2

We used the ward's linkage method to recursively link clusters according to the distance matrix. The ward's linkage method calculates the increase in the total within-cluster sum of squares as a result of joining two clusters. The within-cluster sum of squares is defined as the sum of the squares of the distances between all objects in the cluster and the centroid of the cluster. The sum of squares metric we used is defined as:

$$d(s,r) = \sqrt{\frac{2n_s n_r}{(n_s + n_r)}} ||\tilde{x}_s - \tilde{x}_r||$$

where

$\|\ \|$ is the Euclidean distance.

$\tilde{x}_s$ and $\tilde{x}_r$ are the centroids of clusters r and s.

n_s and n_r are the number of elements in clusters r and s.

We then obtained, as an output from the ward's linkage method, the agglomerative hierarchical cluster tree, returned as a numeric matrix `Z` which is an $(n-1)$-by−3 matrix, where

$$n = number\ of\ random\ numbers\ produced\ in\ temporal\ sequence.$$

Columns 1 and 2 of `Z` contain cluster indices linked in pairs to form a binary tree. The leaf nodes are marked as cluster indices from 1 to n. Leaf

Preprints (www.preprints.org) | NOT PEER-REVIEWED | Posted: 21 April 2022 doi:10.20944/preprints202204.0193.v1

nodes are the singleton clusters from which all higher clusters are built. Each newly formed cluster, corresponding to row `Z(I,:)`, is assigned the index n + `I`. The entries `Z(I,1)` and `Z(I,2)` contain the indices of the two component clusters that form cluster n + `I`. The n– 1 higher clusters correspond to the interior nodes of the clustering tree. `Z(I,3)` contains the linkage distance between the two clusters merged in row `Z(I,:)`.

Step 2. Producing a p-adic scale free dendrogram from an agglomerative hierarchical cluster binary tree.

Step 2.1

Each leaf node of the agglomerative hierarchical cluster binary tree has a path from root to leaf. The leaf path passes m nodes of bifuractions. Each node of bifurcation, in a leaf path, bifurcates right or left. Thus, each leaf path will be represented as a binary string, $branch_r\ r \in 1,2..n\ n = number\ of\ random\ numbers\ produced\ in\ temporal\ sequence$.

- The i'th ($i \in 1,2..m$) position of the binary string will have the value 1 if at the i'th node of bifurcation ($i \in 1,2..m$) the path bifurcates right.
- The i'th ($i \in 1,2..m$) position of the binary string will have the value 0 if at the i'th node of bifurcation ($i \in 1,2..m$) the path bifurcates left.

Step 2.2

All $branch_r$ will be joind to form a matrix D, which represents the p-adic scale free dendrogram with n number of rows and w number of columns where

$$n = umber\ of\ random\ numbers\ produced\ in\ temporal\ sequence$$

$$w = maximal\ i^{'}\ th\ in\ all\ path_r\ with\ the\ value\ 1$$

Each $branch_r$ i'th position that is bigger than its m but smaller or equal to w is filled with the value 0.

Each row in the D matrix which represents a p-adic scale free dendrogram is a string with values of 0/1.

Each such row represents the $j^{'}\ th$ leaf node branch of the p-adic scale free dendrogram, $where\ j \in 1,2..n\ n = number\ of\ discrete\ locations$.

References:

1. Shor, O.; Benninger, F.; Khrennikov, A. Representation of the Universe as a Dendrogramic Hologram Endowed with Relational Interpretation. *Entropy* **2021**, *23*, 584. https://doi.org/10.3390/e23050584.
2. Shor, O.; Benninger, F.; Khrennikov, A. Dendrogramic Representation of Data: CHSH Violation Vs. Nonergodicity. *Entropy* **2021**, *23*, 971. https://doi.org/10.3390/e23080971.
3. Shor, O.; Benninger, F.; Khrennikov, A. Towards Unification of General Relativity and Quantum Theory: Dendrogram Representation of the Event-Universe. *Entropy* **2022**, *24*, 181. https://doi.org/10.3390/e2402018.
4. Wheeler, J.A. Information, Physics, Quantum: The Search for Links. In Proceedings of III International Symposium on Foun-Dations of Quantum Mechanics, Tokyo, Japan, 28–31 August 1989; pp. 354–358.
5. Smolin, L. Einstein's Unfinished Revolution: The Search for What Lies beyond the Quantum; Penguin Press: London, UK, 2019.
6. Smolin, L. The Dynamics of Difference. *Found. Phys.* **2018**, *2*, 643–653.
7. Barbour, J.; Smolin, L. Extremal Variety as the Foundation of a Cosmological Quantum Theory. *arXiv* **1992**. arXiv:Hep-th/9203041.

8. Rovelli, C. Relational Quantum Mechanics. *Int. J. Theor. Phys.* **1996**, *35*, 1637–1678. https://doi.org/10.1007/bf02302261.
9. Barbour, J. *The End of Time*; Oxford University Press: New York, NY, USA, 2000.
10. Barbour, J. The Janus point : a new theory of time; Basic Books: New York, NY, USA, 2020
11. J. Barbour, T. Koslowski, and F. Mercati, A gravitational origin of the arrows of time, arxiv:1310.5167
12. J. Barbour, T. Koslolwski, and F. Mercati, Identification of a gravitational arrow of time, Phys. Rev. Lett. 113:181101 (2014) – arxiv:1409.0917
13. J. Barbour, T. Koslowski, and F. Mercati, Entropy and the typicality of universes, arxiv:1507.06498
14. J. Barbour, "Shape Dynamics. An Introduction," arXiv:1105.0183 [gr-qc].
15. Flavio Mercati, A Shape Dynamics Tutorial, arXiv:1409.0105 [gr-qc]
16. Vladimirov, V.S.; Volovich, I.V.; Zelenov, E.I. *p-Adic Analysis and Mathematical Physics*; World Scientific: Singapore, 1994.
17. Freund, P.G.O.; Witten, E. Adelic string amplitudes. *Phys. Lett. B* **1987**, *199*, 191–194.
18. Parisi, G.. On p-adic functional integrals. *Modern Physics Letters A* **1988**, *3*(06), 639-643.
19. Khrennikov, A. *p-Adic Valued Distributions in Mathematical Physics*; Springer: Berlin/Heidelberg, Germany, 1994.
20. Zelenov, E. I. Entropy gain in p-Adic quantum channels. *Physics of Particles and Nuclei* volume 51, pages 485–488 (2020)
21. Frampton, P.H. Particle theory at Chicago in the late sixties and *p*-Adic strings. *J. Phys. A: Math. Theor.* 2020, **53,** 191001.
22. García-Compeán, H., Edgar Y. López, and W. A. Zúñiga-Galindo. p-Adic open string amplitudes with Chan-Paton factors coupled to a constant B-field. *Nuclear Physics B* 951 (2020): 114904.
23. Dragovich, B. "A p-Adic Matter in a Closed Universe." *Symmetry* 14.1 (2022): 73.
24. Parisi, G.; Sourlas, N. P-adic numbers and replica symmetry breaking. *Eur. Phys. J. B Condens. Matter Complex. Syst.* **2000**, *14*, 535–542.
25. Chen, L.; Liu, X.; Hung, L. Emergent Einstein Equation in P-Adic Conformal Field Theory Tensor Networks. *Phys. Rev. Lett.* **2021**, *127*, 221602. [Google Scholar] [CrossRef]
26. Hung, L.-Y.; Li, W.; Melby-Thompson, C.M. P-Adic CFT is a Holographic Tensor Network. *J. High Energy Phys.* **2019**, *2019*, 170. [Google Scholar] [CrossRef]
27. Gubser, S.S.; Heydeman, M.; Jepsen, C.; Marcolli, M.; Parikh, S.; Saberi, I.; Stoica, B.; Trundy, B. Edge Length Dynamics on Graphs with Applications to P-Adic AdS/CFT. *J. High Energy Phys.* **2017**, *2017*, 1–35. [Google Scholar] [CrossRef]
28. Heydeman, M.; Marcolli, M.; Saberi, I.; Stoica, B. Tensor Networks, P-Adic Fields, and Algebraic Curves: Arithmetic and the AdS_3/CFT_2 Correspondence. *Adv. Theor. Math. Phys.* **2018**, *22*, 7639. [Google Scholar] [CrossRef]
29. Gubser, S.S.; Knaute, J.; Parikh, S.; Samberg, A.; Witaszczyk, P. P-Adic AdS/CFT. *Commun. Math. Phys.* **2017**, *352*, 1019–1059. [Google Scholar] [CrossRef]
30. Khrennikov, A. Yu, Kozyrev, S. V. Replica symmetry breaking related to a general ultrametric space I: replica matrices and functionals. *Physica A: Statistical Mechanics and its Applications* 359 (2006), 222-240.
31. Khrennikov, A. Yu, Kozyrev, S. V. Replica symmetry breaking related to a general ultrametric space—II: RSB solutions and the n→ 0 limit. *Physica A: Statistical Mechanics and its Applications* 359 (2006), 241-266.
32. Khrennikov, A. Yu, Kozyrev, S. V. Replica symmetry breaking related to a general ultrametric space III: The case of general measure. *Physica A: Statistical Mechanics and its Applications* 378.2 (2007), 283-298.
33. Khrennikov, A. Information Dynamics in Cognitive, Psychological, Social and Anomalous Phenomena, Springer-Science + Business Media, B.Y., Dordrecht, NL, 2004.
34. Albeverio S, Khrennikov A and Kloeden P E Memory retrieval as a p-adic dynamical system BioSystems, 49, 105--115 (1999).
35. Khrennikov, A. Modelling of psychological behavior on the basis of ultrametric mental space: Encoding of categories by balls. P-Adic Numbers, Ultrametric Analysis, and Applications, 2, 1-20 (2010).
36. F. Murtagh, Ultrametric model of mind, I: Review. P-adic numbers, Ultrametric Analysis and Applications, 4, 193-206 (2012).
37. F. Murtagh, Ultrametric model of mind, II: Application to text content analysis. P-adic numbers, Ultrametric Analysis, and Applications, 4, 207-221 (2012).
38. Khrennikov, A. Cognitive processes of the brain: An ultrametric model of information dynamics in unconsciousness. P-adic Numbers, Ultrametric Analysis, and Applications, \rm 6, 293-302 (2014).
39. Shor, O., Glik, A., Yaniv-Rosenfeld, A., Valevski, A., Weizman, A., Khrennikov, A., & Benninger, F. (2021). EEG p-adic quantum potential accurately identifies depression, schizophrenia and cognitive decline. *Plos one*, *16*(8), e0255529.

40. Palmer T. N. Discretization of the Bloch sphere, fractal invariant sets and Bell's theorem*Proc. R. Soc. A.* 2020 , **476,** 20190350.
41. Hossenfelder S and Palmer T Rethinking Superdeterminism. *Front. Phys.* 2020, 8, 139.
42. Atmanspacher, H. Determinism is ontic, determinability is epistemic. In *Between Chance and Choice: Interdisciplinary Perspectives on Determinism*; Atmanspacher, H., Bishop, R.C., Eds.; Imprint Academic: Thorverton, UK, 2002; pp. 49–74. [Google Scholar]
43. Atmanspacher, H.; Primas, H. Epistemic and ontic quantum realities. In *Time, Quantum and Information*; Castell, L., Ischebeck, O., Eds.; Springer: Berlin/Heidelberg, Germany, 2003. [Google Scholar]
44. Hertz, H. *The Principles of Mechanics: Presented in a New Form*; Macmillan: London, UK, 1899. [Google Scholar]
45. Boltzmann, L. Uber die Frage nach der objektiven Existenz der Vorgnge in der unbelebten Natur. In *Populre Schriften*; Barth, J.A., Ed.; Springer: Leipzig, Germany, 1905. [Google Scholar]
46. Khrennikov, A. Quantum epistemology from subquantum ontology: Quantum mechanics from theory of classical random fields. *Ann. Phys.* **2017**, *377*, 147–163. [Google Scholar] [CrossRef]
47. Khrennikov, A. Hertz's Viewpoint on Quantum Theory. *Act. Nerv. Super.* **2019**, *61*, 24–30. [Google Scholar] [CrossRef]